PROCEEDINGS OF SCIENCE

Testing Hadronic Interaction models with Muon Densities from KASCADE-Grande Data

A.L. Colmenero-César*[a], J.C. Arteaga-Velázquez[a], M. Bertaina[b], A. Chiavassa[b], K. Daumiller[c], V. de Souza[d], R. Engel[c,e], A. Gherghel-Lascu[f], C. Grupen[g], A. Haungs[c], J.R. Hörandel[h], T. Huege[c], K.-H. Kampert[i], D. Kang[c], K. Link[c], H.J. Mathes[c], S. Ostapchenko[j], T. Pierog[c], D. Rivera-Rangel[a], M. Roth[c], H. Schieler[c], F.G. Schröder[c], O. Sima[k], A. Weindl[c], J. Wochele[c], J. Zabierowski[l]

[a] *Universidad Michoacana, Instituto de Física y Matemáticas, Morelia, Mexico*
[b] *Dipartimento di Fisica, Università degli Studi di Torino, Italy*
[c] *Karlsruhe Institute of Technology, Institute for Astroparticle Physics, Germany*
[d] *Universidade São Paulo, Instituto de Física de São Carlos, Brasil*
[e] *Karlsruhe Institute of Technology, Institute of Experimental Particle Physics, Germany*
[f] *Horia Hulubei National Institute of Physics and Nuclear Engineering, Bucharest, Romania*
[g] *Department of Physics, Siegen University, Germany*
[h] *Dept. of Astrophysics, Radboud University Nijmegen, The Netherlands*
[i] *Fachbereich Physik, Universität Wuppertal, Germany*
[j] *Hamburg University, II Institute for Theoretical Physics, 22761 Hamburg*
[k] *Department of Physics, University of Bucharest, Bucharest, Romania*
[l] *National Centre for Nuclear Research, Department of Astrophysics, Lodz, Poland*
*Speaker, Email:1615807e@umich.mx

The study of the muon content in extensive air showers (EAS) is relevant for understanding the origin and nature of cosmic rays. Moreover, muons serve as a sensitive observable to hadronic interactions in air showers, offering insight into high-energy physics processes. However, discrepancies between measured and predicted shower muon content have been reported by some EAS observatories, hinting to deficiencies of high-energy hadronic interaction models. In this work, we study the muon content of EAS with KASCADE-Grande data for primary energies between 10 PeV and 1 EeV, considering showers with zenith angles of $\theta \leq 40^{\circ}$. In particular, we estimate the local muon density at fixed radial distances from the shower core and explore its dependence on atmospheric depth. Adapting the energy scale from the Pierre Auger Observatory (PAO) we compare the data against predictions of the QGSJet-II-04, EPOS-LHC and SIBYLL-2.3d hadronic interaction models. While good agreement is found in a large parameter space, a discrepancy between the measured and predicted local muon densities can be seen, especially for high primary energies and vertical events and here increasing for large radial distances of the measured muons from the EAS core. This could indicate an inadequate description of the attenuation of muons in the atmosphere.

39th International Cosmic Ray Conference (ICRC2025)
15–24 July 2025
Geneva, Switzerland

ICRC 2025
The Astroparticle Physics Conference
Geneva July 15-24, 2025

https://pos.sissa.it/

PoS(ICRC2025)224

1. Introduction

Extensive air showers of hadronic origin, i.e. produced by cosmic-ray collisions in the Earth's atmosphere, are composed by electrons, muons, photons, hadrons and atomic nuclei, whose relative abundances, energy spectra and space-time distributions are sensitive to the mass, charge and energy of the primary cosmic-ray particle [1]. A study of these observables with ground-based shower detectors allows to extend the investigations of cosmic rays beyond 10 TeV and to investigate the properties of hadronic collisions at energies not reachable by modern particle physics accelerators. It also opens the possibility of testing models on high-energy hadronic interactions with data of EAS detectors [2]. One EAS component that is important to analyze and understand due to its sensitivity to the cosmic-ray composition and to the properties of hadronic interactions is the muon cascade. In the last years, several experiments have reported differences between the measurements and the predictions of the post-LHC hadronic interaction models on the muon content of EAS [3]. The Pierre Auger (875 $\mathrm{g/cm^2}$ of atmospheric overburden), for example, has reported an excess of muons in comparison with the expectations at ultra-high energies [4, 5]. Previous measurements of KASCADE-Grande (1022 $\mathrm{g/cm^2}$ of atmospheric depth) on the muon size of EAS for energy thresholds of $E_\mu > 230$ MeV (vertical incidence) as a function of the zenith angle have also find discrepancies with MC simulations, in particular that the attenuation length of muons is larger than the predictions of the post-LHC hadronic interaction models QGSJet-II-04 and EPOS-LHC [6]. In addition, if the primary energy in KASCADE-Grande data is calibrated using the energy scale of the PAO then the muon excess is not observed [7]. Since muons are measured at various energy thresholds, observation levels, and radial distances from the shower core, it should be noted that comparing the results of various experiments can be difficult. To further investigate these results in KASCADE-Grande, here, we have performed an analysis of the mean muon density in hadronic air showers using the data of the detector at radial distances from 300 to 600 m from the shower axis in shower coordinates. We studied the muon densities as a function of the primary energy, calibrated to the energy scale of the PAO. To explore the dependence on atmospheric depth, the data were divided into three zenith angle intervals: $[0.0°, 21.78°)$, $[21.78°, 31.66°)$, and $[31.66°, 40.0°]$.

2. The KASCADE-Grande Experiment

The KASCADE-Grande cosmic-ray experiment was situated on the Campus North of the Karlsruhe Institute of Technology (49.1° N, 8.4° E) in Karlsruhe, Germany, at a height of 110 meters above sea level [8]. The electromagnetic, muon, and hadron components of EAS originated by cosmic rays with primary energy ranging from 1 PeV to 1 EeV were measured by a complex of different systems of particle detectors. A calorimeter, scintillator and muon detector array, multi-wire proportional chambers, underground tracking detectors, and streamer tubes were among the various detector types that made up the original design of the experiment. The primary detection systems of the experiment were the Grande and KASCADE arrays (see Fig. 1, left). The primary array of KASCADE was made up of a $200 \times 200\ \mathrm{m^2}$ square grid of 252 liquid scintillator detectors arranged 13 m apart from each other and grouped into 16 detector clusters. It was used to monitor shower electrons and photons (with a threshold energy of 5 MeV for vertical incidence). In contrast, a set of 192 shielded plastic scintillator detectors situated below the electromagnetic detector units of the outer clusters of the KASCADE array were used to detect shower muons with energies $E > 230$ MeV for vertical incidence. The Grande array was composed of 37 particle scintillator detector units distributed over an area of 0.5 km^2 and provided measurements of charged particles, the direction of the shower and the EAS core position. The total number of shower electrons (N_e), muons (N_μ), and charged particles (N_{ch}) were measured event by event using the combined shielded and unshielded detectors from KASCADE and the scintillator detectors from Grande.

3. KASCADE-Grande Data

The dataset comprises 1.276×10^7 events collected over almost nine years with the KASCADE-Grande air shower array. Events were selected using cuts from previous analyses [7] to reduce systematic uncertainties. This selection includes showers that were successfully reconstructed and that were measured during stable runs for which neither hardware problems nor anomalies in the energy deposits at the Grande stations were observed. We also chose events with zenith angles smaller than 40°, with reconstructed EAS cores located in a central fiducial area within Grande at radial distances from the KASCADE center between 150 and 650 m. To be included in the selected data sample, EAS events must have muon sizes $N_\mu > 3 \times 10^4$, electron numbers $N_e > 1.1 \times 10^4$, shower ages in the interval $[-0.385, 1.485]$ and more than 11 triggered Grande stations. In KASCADE-Grande, the measured muon densities ρ_μ are provided for radial bins of $\Delta r = 20$ m width at shower disk coordinates. For this analysis, we only kept events which have ρ_μ data within radial distance intervals around $r = 600$, 500, 400 and 300 m.

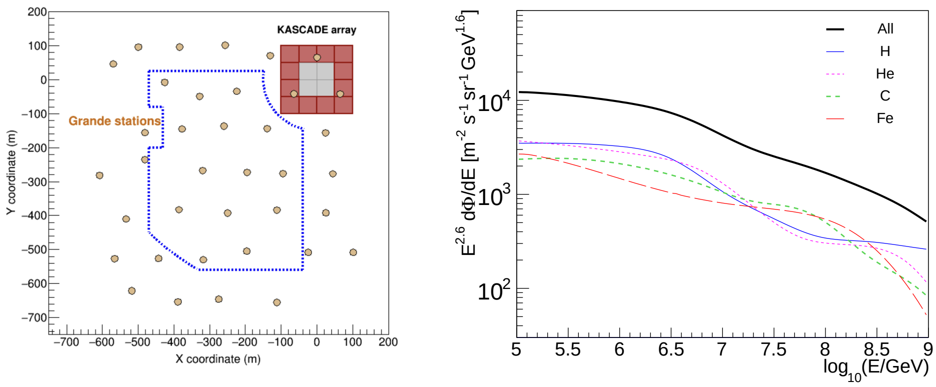

Figure 1: Left: Schematic layout of the KASCADE-Grande detector. Circles denote the Grande stations, squares in the upper right-hand side indicate the KASCADE array. The analysis region is outlined by the blue dashed line [7]. **Right:** Energy spectra for the H, He, C and Fe mass groups of cosmic rays for the cosmic-ray nominal composition model used in this work (GFS model with an energy shift which allows to match its total energy spectrum with that of the Pierre Auger Observatory [15]).

4. Monte-Carlo Simulations

Monte-Carlo (MC) simulations were performed using CORSIKA v7.5 [9], considering the following primary nuclei: H, He, C, Si, and Fe. Hadronic interactions at $E_h < 200$ GeV were

PoS(ICRC2025)224

simulated with Fluka 2011.2 [10] and, at higher energies, with QGSJet-II-04 [11], EPOS-LHC [12], and SIBYLL 2.3d [13]. The primary spectra follow an E^{-2} power law. Showers were produced with primary energies in the interval from $E = 10^{15}$ to 3.16×10^{18} eV. A detailed detector simulation is carried out with GEANT for each CORSIKA shower generated. As a cosmic-ray composition model, we adopted the GSF model [14], which was simulated by introducing appropriate weights to the data. An energy shift ($E = 0.9328 \times E_{GSF}$) was also applied to the MC simulations to match the total spectrum of the model with the one measured with the PAO [15]. This procedure was done to calibrate our cosmic-ray model with the PAO energy scale. The energy spectra from our nominal composition model are plotted in the right panel of Fig. 1.

5. Analysis Method

To estimate the muon density at a specific radial distance r for a given shower event, we used the corresponding N_μ value provided by the KASCADE-Grande database along with the muon lateral distribution function (LDF) defined in [8]:

$$\rho_\mu(r) = N_\mu \cdot \frac{0.28}{r_0^2} \left(\frac{r}{r_0}\right)^{p_1} \left(1 + \frac{r}{r_0}\right)^{p_2} \left(1 + \left(\frac{r}{10 \cdot r_0}\right)\right)^{p_3}, \tag{1}$$

which was used to estimate the shower muon size of the event from the measured muon densities by means of a maximum likelihood procedure. In the above equation, $p_1 = -0.60$, $p_2 = -2.39$, $p_3 = -1.0$ and $r_0 = 320$ m, according to [8]. For the main analysis, the muon density was calculated event-by-event at $r = 600$ m. This quantity will be referred to as $\rho_\mu(600)$. Fig. 2 displays the muon densities for a individual Monte-Carlo event compared with the corresponding muon LDF given by eq. (1).

To estimate $\rho_\mu(600)$ as a function of the primary energy, we adopted the procedure introduced by the NEVOD-DECOR [16] and SUGAR [17] collaborations. This method compares the measured $\rho_\mu(600)$ distribution $dN/d\rho_\mu^{exp}(600)$ with the predicted one, $dN/d\rho_\mu^{MC}(600)$, by a reference cosmic ray model, which is the nominal model already described above that is calibrated with the energy scale of the PAO. Assuming that the expected distribution must coincide with the experimental histogram, the predicted $\rho_\mu^{MC}(600)$ values in the reference model are then modified by an appropriate factor R_μ, which depends on the primary energy, to reproduce $dN/d\rho_\mu^{exp}(600)$. From this procedure, we estimated $R_\mu = d\rho_\mu^{exp}(600)/d\rho_\mu^{MC}(600)$ and applied it to the Monte Carlo simulations. The factor R_μ and the expected and measured distributions

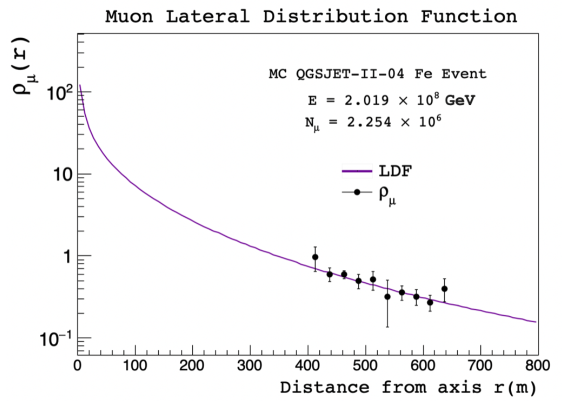

Figure 2: Muon densities (dots) for a Monte-Carlo event (QGSJet-II-04) generated by a Fe primary compared to the respective reconstructed muon lateral distribution function (solid line).

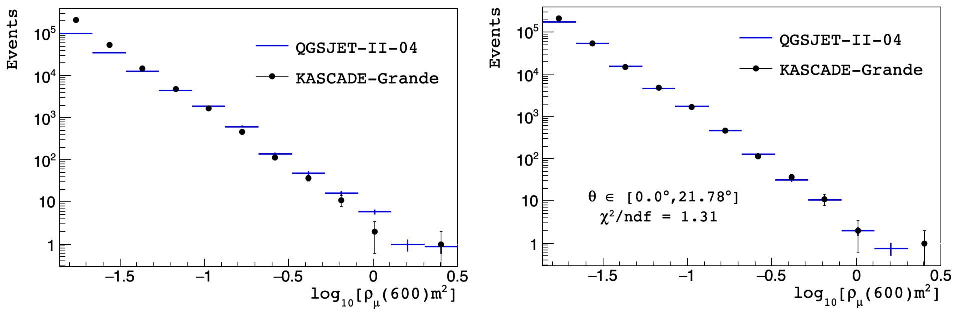

Figure 3: Both panels show histograms of the same dataset: **Left:** experimental muon densities (dots) and the corresponding QGSJet-II-04 predictions (lines) at 600 m for vertical events ($\theta < 21.78°$). **Right:** Results after applying the χ^2 fitting procedure, including the resulting χ^2/ndf.

are related by means of the following equation:

$$\begin{aligned} dN[\rho_\mu^{exp}(600)]/d\rho_\mu^{exp}(600) &= dN[\rho_\mu^{MC}(600)]/d\rho_\mu^{MC}(600) \times d\rho_\mu^{MC}(600)/d\rho_\mu^{exp}(600) \\ &= dN[\rho_\mu^{exp}(600)/R]/d\rho_\mu^{MC}(600) \times 1/R. \end{aligned} \tag{2}$$

By plotting the mean $R_\mu \rho_\mu^{MC}(600)$ vs E, we then provide an estimate of the muon density content in KASCADE-Grande as a function of the primary energy. This approach was chosen because KASCADE-Grande lacks of an energy scale independent of simulations.

To obtain the factor R_μ, first, we constructed a histogram for $\log_{10}\rho_\mu(600)$ for each zenith angle interval for both the measured data and the nominal MC model. The histogram range spans from -2.25 to 0.5 and was divided into $m = 14$ bins, resulting in a bin width of approximately 0.2. As an example, the left panel of Fig. 3 displays the measured histogram for vertical events alongside the predicted distribution from QGSJet-II-04 using our nominal cosmic-ray composition model.

Next, the factor R_μ is parameterized, in logarithmic scale, using the piecewise parabolic function

$$\delta_\mu(E;\mathbf{a}) = \log_{10}[R_\mu(E;\mathbf{a})] = \begin{cases} a_0 + a_1 \cdot (\log_{10} E - 8.0) + a_2 \cdot (\log_{10} E - 8.0)^2, & \log_{10} E \leq 8.0, \\ a_0 + a_1 \cdot (\log_{10} E - 8.0) + a_3 \cdot (\log_{10} E - 8.0)^2, & \log_{10} E > 8.0, \end{cases} \tag{3}$$

where $\mathbf{a} = (a_0, a_1, a_2, a_3)$ is a vector that contains the free parameters of the formula and E is expressed in GeV. The a_i parameters are obtained with the minimum χ^2 method:

$$\chi^2 = \sum_{i=1}^{m} \left(\frac{N_{exp,i} - N_{MC,i}(\mathbf{a})}{\sigma_{MC,i}} \right)^2, \tag{4}$$

in such a way that the predicted $\rho_\mu(600)$ histogram is able to match the measured distribution. In the above equation $N_{exp,i}$ is the number of events at the i-bin of the measured distribution, $N_{MC,i}(\mathbf{a})$ is the expected number of events at the same bin after applying the factor R_μ to the MC simulations, while $\sigma_{MC,i}$ is the corresponding statistical error.

Once, the best-fit $\mathbf{a}$ parameters are obtained, the corresponding correction $\delta_\mu(E;\mathbf{a})$ is calculated and is then applied to the MC densities in the following way:

$$\log_{10}\hat{\rho}_\mu(600) = \log_{10}\rho_\mu^{MC}(600) + \delta_\mu(E;\mathbf{a}). \tag{5}$$

Here, E is known from MC simulations. $\hat{\rho}_\mu(600)$ represents our estimation of the experimental muon density. The right panel of Fig. 3 shows, as an example, the muon density histograms after performing the fitting procedure with the QGSJet-II-04 model. With the MC data sets already calibrated, we estimated the mean $\hat{\rho}_\mu(600)/E$ in KASCADE-Grande versus the primary energy.

6. Results

For each high-energy hadronic interaction model and zenith angle interval, we compute the mean of $\hat{\rho}_\mu(600)/E$ as a function of the logarithm of the primary energy $\log_{10}(E)$. The results are shown in Fig. 4. They are compared with the original model predictions for pure protons and iron nuclei, as well as for a mixed composition scenario, which was estimated with our nominal cosmic-ray composition model. The data are shown with statistical errors and systematic uncertainties. The statistical errors are estimated by varying the fitted parameters within their 68% confidence level interval. The systematic errors include the uncertainties on the energy scale of the PAO [15], which was evaluated by modifying the energy scale of the nominal model by ±14%, and the relative abundances of cosmic rays. The latter was estimated by increasing/reducing the relative abundance of the heavy (C+Fe) to light (H+He) nuclei by the factors 1.83 and 0.62 in the model to have relative abundances as those found in [18]. The systematic errors were added in quadrature.

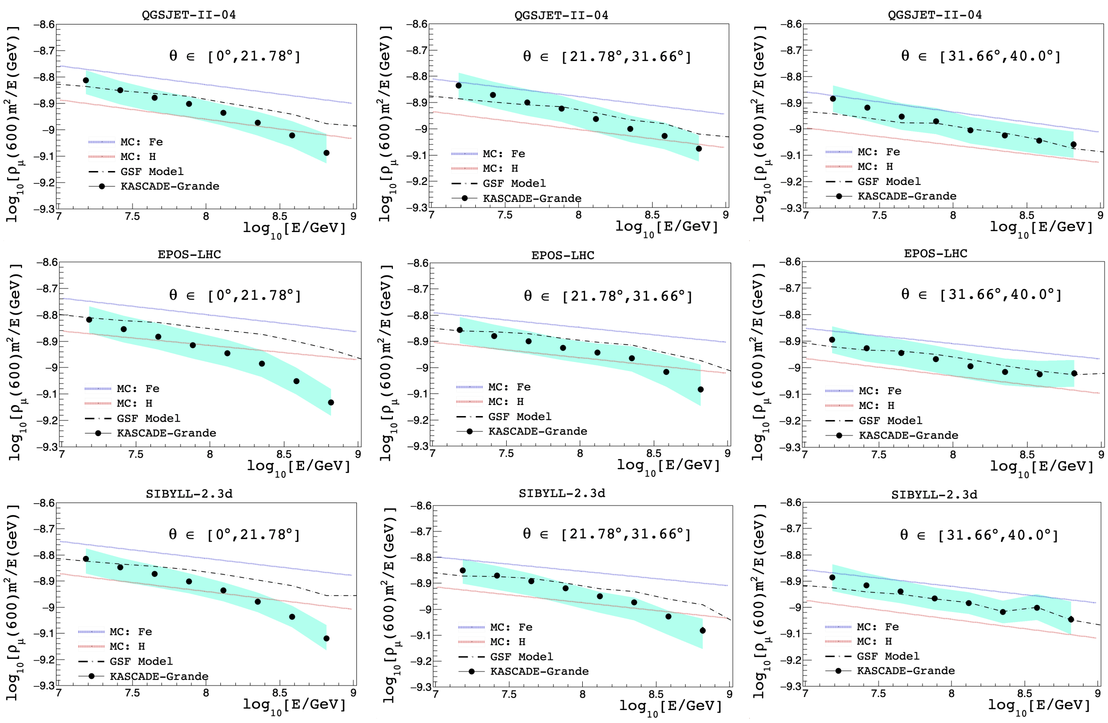

Figure 4: Experimental data (circles) and predictions for the QGSJet-II-04, EPOS-LHC and SIBYLL 2.3d model (lines) for $\log_{10}[\rho_\mu(600)/E]$ as a function of $\log_{10} E$. Each column corresponds to a zenith angle interval, and each row to a different hadronic interaction model. The blue line represents Fe predictions, the red lines, proton expectations, and the middle dotted line the prediction from the nominal cosmic-ray model. Vertical error bars indicate the statistical uncertainties, the teal band the total systematic uncertainty.

From the plots in Fig. 4, we observe that, for $\theta < 21.78°$, our muon density estimations from the KASCADE-Grande measurements, calibrated with the PAO energy scale, are within the predictions of the hadronic interaction models QGSJet-II-04, EPOS-LHC and SIBYLL 2.3d for protons and iron primaries at energies between 10^{16} eV and 10^{17} eV. At higher energies, where it is expected that the heavy component dominates the composition, the KASCADE-Grande results for $\hat{\rho}_\mu(600)$ at sea level are overestimated by the hadronic interaction models, more significant for EPOS and SIBYLL than for QGSJet. This discrepancy becomes smaller at larger zenith angels and vanishes for the third zenith angular range.

As a consequence, if we compare the estimated $\hat{\rho}_\mu(600)$ with the predictions of the nominal cosmic-ray composition model, we observe a disagreement between the experimental estimations and the expectations for vertical showers, which increases with the primary energy and decreases with the zenith angle. For inclined showers, the predictions of the nominal model are in good agreement with the $\hat{\rho}_\mu(600)$ estimations.

Therefore, it can be concluded that the evolution of the atmospheric depth of the muon density estimated from the KASCADE-Grande data is probably not well described by the models of the high-energy hadronic interaction, since the experimental data show a lower atmospheric attenuation compared to the simulations. This result is independent of the energy scale considered. The KASCADE-Grande collaboration reported a similar behavior for the muon number N_μ in hadronic-induced air showers [6].

As a further test, we have investigated the muon densities for inclined and vertical showers for three additional radial distances using the QGSJet-II-04 model. It can be seen (Fig. 5) that the agreement tends to improve closer to the shower core. That is, the MC overestimation of the muon density increases at larger distances, supporting a deficiency in the shape of the muon LDF for hadronic air showers.

In addition, we studied effects on the results by the systematic uncertainties in azimuth (due to the EAS-asymmetric measurements of the muons at KASCADE-Grande), zenith angle and shower core reconstruction. Some variations have been observed in $\hat{\rho}_\mu(600)$ close to 1 EeV, which may

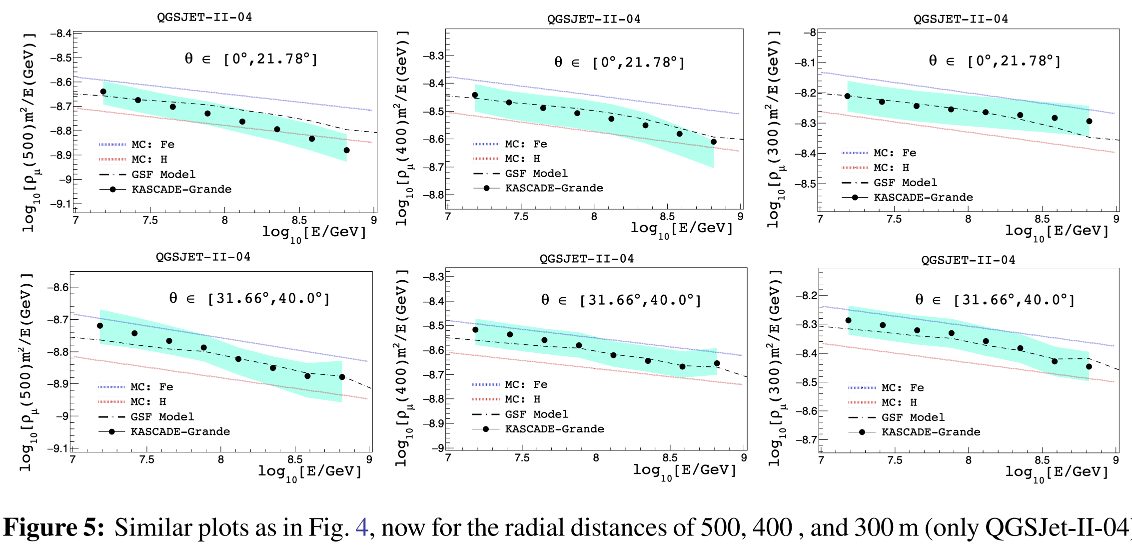

Figure 5: Similar plots as in Fig. 4, now for the radial distances of 500, 400 , and 300 m (only QGSJet-II-04). Each column corresponds to a fixed radial distance, and each row to a given zenith angle interval.

increase the systematic uncertainty band at highest energies, but does not change the general picture. Further investigations in this direction are ongoing.

7. Conclusions

The density of muons at sea-level with an energy threshold of 230 MeV, measured by KASCADE-Grande at radial distances from 300 to 600 m from the shower core, were analyzed and compared to the predictions from the hadronic interaction models QGSJet-II-04, EPOS-LHC and SIBYLL 2.3d in the energy range from 10 PeV to 1 EeV and for zenith angles smaller than 40°. A good agreement is observed for inclined showers at all lateral distances; however, in the case of more vertical showers at high primary energies, the data reveal a deficit of low-energy muons at large distances relative to the Monte-Carlo predictions. This discrepancy is reduced when compared to muons located closer to the shower core. This hints to a mismatch in the attenuation of the muons with the atmospheric depth. The origin of these findings are not related with systematic errors in the reconstruction of the arrival direction and the core position of the EAS, as well as not by the assumption of a certain composition model or the energy scale of the primary cosmic ray spectrum. In addition to hitherto unexamined systematic uncertainties, the source of the disagreement might be related with the predicted muon energy spectrum and/or the muon lateral distribution. Further studies are ongoing, and can also be performed by the public as all the KASCADE-Grande data is publicly available via KCDC [19, 20].

Acknowledgements

J.C.A.V. and A.L.C.C. wants to thank the partial support from CONACYT (grant A1-S-46288) and SECIHTI.

References

[1] P.K.F. Grieder, Extensive Air Showers, High Energy Phenomena and Astrophysical Aspects - a tutorial, reference manual and data book, Vol. I and II, (2010), Springer.
[2] R. Engel et al., Annu. Rev. Nucl. Part. Sci. 61, (2011) 467.
[3] J.C. Arteaga-Velazquez et al., PoS (ICRC2023) 466, 2023.
[4] A. Aab et al., Pierre Auger Collab., Phys. Rev. D 91, (2015) 032003.
[5] A. Aab et al., Pierre Auger Collab., Phys. Rev. Lett. 117, (2016) 192001.
[6] W. D. Apel et al., Astropart. Phys. 95, (2017) 25.
[7] J.C. Arteaga-Velazquez et al., PoS (ICRC2023) 376, 2023.
[8] W. D. Apel et al., NIMA 620, (2010) 202.
[9] D. Heck et al., Report No. FZKA 6019, Forschungszentrum Karlsruhe-Wissenschaft Berichte (1998).
[10] G. Battistoni et al., Annals of Nuclear Energy 82, (2015) 10.
[11] S. Ostapchenko, Phys. Rev. D 83, (2011) 014018.
[12] T. Pierog et al., Phys. Rev. C 92, (2015) 034906.
[13] F. Riehn et al., Phys. Rev. D 102, (2020) 063002.
[14] H. Dembinski et al., PoS (ICRC2017) 533, 2017.
[15] V. Verzi et al., Pierre Auger Collab., ICRC 2019, PoS (ICRC2019) 450.
[16] A. Bogdanov et al., Astrop. Phys. 98, (2018) 13.
[17] J. Bellido et al., Phys. Rev. D 98, (2018) 023014.
[18] J.C. Arteaga-Velázquez et al., EPJ Web of Conf. 172, (2018) 07003.
[19] https://kcdc.iap.kit.edu/.
[20] A. Haungs, *et al.*, Eur. Phys. J. C **78** (2018) no.9, 741.

PoS(ICRC2025)224